The Journal of Immunology

Complement Regulatory Protein Factor H Is a Soluble Prion Receptor That Potentiates Peripheral Prion Pathogenesis

Sarah J. Kane, Taylor K. Farley, Elizabeth O. Gordon, Joshua Estep, Heather R. Bender, Julie A. Moreno, Jason Bartz, Glenn C. Telling, Matthew C. Pickering and Mark D. Zabel

J Immunol 2017; 199:3821-3827; Prepublished online 25 October 2017;
doi: 10.4049/jimmunol.1701100
http://www.jimmunol.org/content/199/11/3821

The Journal of Immunology is published twice each month by
The American Association of Immunologists, Inc.,
1451 Rockville Pike, Suite 650, Rockville, MD 20852

Print ISSN: 0022-1767 Online ISSN: 1550-6606.

Complement Regulatory Protein Factor H Is a Soluble Prion Receptor That Potentiates Peripheral Prion Pathogenesis

Sarah J. Kane,* Taylor K. Farley,*,† Elizabeth O. Gordon,* Joshua Estep,* Heather R. Bender,* Julie A. Moreno,* Jason Bartz,‡ Glenn C. Telling,* Matthew C. Pickering,§ and Mark D. Zabel*

Several complement proteins exacerbate prion disease, including C3, C1q, and CD21/35. These proteins of the complement cascade likely increase uptake, trafficking, and retention of prions in the lymphoreticular system, hallmark sites of early prion propagation. Complement regulatory protein factor H (fH) binds modified host proteins and lipids to prevent C3b deposition and, thus, autoimmune cell lysis. Previous reports show that fH binds various conformations of the cellular prion protein, leading us to question the role of fH in prion disease. In this article, we report that transgenic mice lacking *Cfh* alleles exhibit delayed peripheral prion accumulation, replication, and pathogenesis and onset of terminal disease in a gene-dose manner. We also report a biophysical interaction between purified fH and prion rods enriched from prion-diseased brain. fH also influences prion deposition in brains of infected mice. We conclude from these data and previous findings that the interplay between complement and prions likely involves a complex balance of prion sequestration and destruction via local tissue macrophages, prion trafficking by B and dendritic cells within the lymphoreticular system, intranodal prion replication by B and follicular dendritic cells, and potential prion strain selection by CD21/35 and fH. These findings reveal a novel role for complement-regulatory proteins in prion disease. ***The Journal of Immunology*****, 2017, 199: 3821–3827.**

Prions encipher and transmit pathogen information via structural conversion of the soluble cellular prion protein (PrP^C) to the misfolded, aggregated pathologic prion protein (PrP^{Sc}). Examples of prion diseases include Creutzfeldt–Jakob disease in humans; scrapie in sheep and goats; bovine spongiform encephalopathy in cattle; chronic wasting disease in deer, elk, and moose; and transmissible mink spongiform encephalopathy (TME) in mink. Hallmark clinical signs of prion diseases can include dementia, ataxia, and weight loss. Neuropathological manifestations of prion disease include astrogliosis, spongiform degeneration, and prion amyloid deposition. Many prion strains, including mouse-adapted scrapie strain RML5 and one TME strain, Hyper (HY), propagate in lymphoid tissues during a clinically silent carrier phase prior to neuroinvasion and clinical manifestations. Interestingly, bovine spongiform encephalopathy and another TME prion strain, Drowsy (DY), lack this phenotype, implicating alternate routes to the CNS independent of lymphoid propagation (1, 2).

The (in)ability of certain prions to breech species barriers, as well as distinct biochemical and pathological characteristics among prions derived from the same PrP^C primary sequence (2, 3), suggests that prions can exist as different strains or quasi-species. However, whether these prion strains arise from enhanced thermodynamic stability of certain conformations in the original inoculum or host factors that preferentially promote certain prion conformations remains inconclusive. Interestingly, prions derived from spleen display broader species tropism compared with prions from brain (4). These data highlight the capacity of strain selection within a single host and suggest that certain host factors likely select for certain prion strains during the transition between establishing infection in extraneural tissues and ultimate neuroinvasion. However, whether selection occurs at the protein conformational level, posttranslational modification status, protein–protein interactions, or cell-type level remains unknown.

Several elegant studies implicate the complement system as a facilitator of early prion propagation and spread. CD21/35- and PrP^C-expressing follicular dendritic cells and B cells capture pathogens opsonized with C3 and C4 cleavage products, decreasing the threshold to activate B cells to induce Ab production. Both follicular dendritic cells and B cells promote prion disease (5–11). Many studies suggest that complement promotes trafficking of infectious prions to cells expressing PrP^C, a substrate for prion replication, in lymphoid follicles. Specifically, mice deficient in C3, C4, C1q, and complement receptors CD21/35 accumulate less splenic prions early in disease and partially or completely resist terminal disease (7, 9–13).

Considering that complement effector proteins can bind host cell surfaces, hosts require regulatory mechanisms to prevent

*Prion Research Center, Department of Microbiology, Immunology, and Pathology, College of Veterinary Medicine and Biomedical Sciences, Colorado State University, Fort Collins, CO 80523; †National Institute of Arthritis and Musculoskeletal and Skin Diseases, National Institutes of Health, Bethesda, MD 20892; ‡School of Medicine, Creighton University, Omaha, NE 68178; and §Department of Medicine, Centre for Complement and Inflammation Research, Imperial College, London W12 0NN, United Kingdom

ORCIDs: 0000-0002-6072-5682 (S.J.K.); 0000-0002-1153-0192 (M.C.P.); 0000-0002-2666-9197 (M.D.Z.).

Received for publication July 31, 2017. Accepted for publication September 29, 2017.

This work was supported by National Institutes of Health National Institute of Neurological Disorders and Stroke Grants R01NS056379-02 and F31NS087762 and by National Institute of Allergy and Infectious Diseases Grant R56AI122273.

The content is solely the responsibility of the authors and does not necessarily represent the official views of the National Institutes of Health.

Address correspondence and reprint requests to Prof. Mark D. Zabel, Prion Research Center, Department of Microbiology, Immunology, and Pathology, College of Veterinary Medicine and Biomedical Sciences, Colorado State University, 1619 Campus Delivery, Fort Collins, CO 80523. E-mail address: Mark.Zabel@colostate.edu

Abbreviations used in this article: dpi, day postinfection; DY, Drowsy; fH, factor H; GFAP, glial fibrillary acidic protein; HY, Hyper; NBH, normal brain homogenate; PK, proteinase K; PMCA, protein misfolding cyclic amplification; PrP^C, cellular prion protein; PrP^{Sc}, pathologic prion protein; rPrP, recombinant prion protein; rpu, relative PMCA unit; SCR, short consensus repeat; sPMCA, serial protein misfolding cyclic amplification; SPR, surface plasmon resonance; TME, transmissible mink spongiform encephalopathy.

self-recognition and subsequent autoimmunity. Complement regulatory protein factor H (fH; β1H globulin or CFH) prevents complement activation on host tissues by binding sialic acids and polyanionic carbohydrates, such as glycosaminoglycan, which are largely absent on pathogen surfaces. Although C3b marks virtually all cell surfaces in circulation, fH bound to host polyanionic carbohydrates mediates C3b inactivation through cofactor activity with factor I, as well as limits activity of the C3 convertase C3bBb (14). Mutations or deficiency in fH lead to autoimmune diseases, such as membranoproliferative glomerulonephritis, atypical hemolytic uremic syndrome, and age-related macular degeneration (15–17).

PrP^{C} and PrP^{Sc} contain sialic acid residues, and splenic PrP^{Sc} is more sialylated than brain PrP^{Sc} (18). Furthermore, fH binds various conformations of recombinant PrP^{C}, suggesting that fH potentially impacts prion disease outcomes (19, 20). Collectively, these previous findings led us to investigate the role of fH in a mouse model of scrapie.

Inactivation of the *Cfh* gene renders mice deficient in plasma C3 [(15) and confirmed in serum of mice reported in this article; data not shown]. Because C3 promotes prion disease (9, 12, 13), its absence in mice also lacking fH confounds the ability to assess the role of fH in prion pathogenesis. To ascertain the specific effect of fH deficiency, we peripherally inoculated mice with a high dose of RML5 mouse-adapted scrapie prions previously shown to affect C3-deficient mice nearly identically to wild-type mice (9). Transgenic mice expressing zero, one, or two allelic copies of *Cfh* exhibited a gene-dose effect of early prion accumulation and onset of terminal disease after challenge with a high dose of RML5 prions. Knockout and hemizygous mice accumulated fewer splenic and brain prions at early time points and resisted the onset of terminal disease in comparison with their fH-sufficient cohorts. We confirmed a direct interaction between fH and recombinant prion protein (rPrP) using surface plasmon resonance (SPR) and, for the first time, to our knowledge, demonstrate that fH interacts with prion amyloid enriched from prion-infected brain. Overall, these surprising data demonstrate that fH may play a direct role in prion disease by promoting certain prion strains' lymphotropism and subsequent neuroinvasion.

Materials and Methods

Mice

All mice were bred and maintained at Lab Animal Resources, accredited by the Association for Assessment and Accreditation of Lab Animal Care International and approved on January 14, 2016 by the Institutional Animal Care and Use Committee at Colorado State University. fH-deficient mice on the C57BL/6 background were kindly provided by Dr. J. Thurman (University of Colorado–Denver). We crossed $Cfh^{-/-}$ mice to hemizygosity with C57BL/6 wild-type mice from The Jackson Laboratory. Hemizygous breeders generated pups of various *Cfh* genotypes.

Genotyping transgenic mice

We determined *Cfh* genotype from DNA extracted from tail clips (69504; QIAGEN) using the following primers: 5′-CTACAAATGCCGCCCTGGAT-3′ (mzBAP3), 5′-CTGCCAGCCTAAAGGACCC-3′ (mzBAP4r), 5′-GTAAAGG TCCTCCTCCAAGAG-3′ (fHReg200), and 5′-GGGGATCGGCAATAAA AAGAC-3′ (NEO). mzBAP3 and mzBAP4r primers were designed using the National Center for Biotechnology Information's primer design Web site and blasted against the available C57BL/6 genome to ensure specificity. PCR conditions were as follows for 35 cycles: denaturation at 95°C, annealing at 55°C, and elongation at 72°C. PCR products were resolved using agarose gel electrophoresis. Amplicons of 400 bp (fHReg200 and NEO) indicated the presence of a knockout allele, and amplicons of 451 bp (BAP3/4) indicated the presence of a wild-type allele.

Mouse inoculations

Age- and sex-matched mice ($n \geq 6$ per genotype), ranging from 6 wk to 1 y, received 100 μl ~ 10^6 LD_{50} units of mouse-adapted scrapie strain RML5 prions i.p. or uninfected normal brain homogenate (NBH) i.p. as mock infection controls.

Clinical scoring

Mice were monitored daily and sacrificed at the onset of terminal disease or specified time points. We used a composite scoring system to assess the severity of disease, including tail rigidity (0–2), akinesia (0–4), ataxia (0–4), tremors (0–4), and weight loss (0–2). Mice scored above 10 (or 4 in any category) were euthanized via CO_2 inhalation, replacing 20% of air per minute to effect.

Tissue collection and analysis

After euthanasia, the following samples were collected and frozen or fixed in 4% formaldehyde in 1× PBS: serum, spleen (half fixed, half frozen), kidneys (one fixed, one frozen), tail clip, and brain (half fixed, half frozen). We assessed the presence of protease-resistant prions (PrP^{Sc}) in 10% (w/v) homogenate after proteinase K (PK; Roche) digestion (10 μg/ml for spleen and 50 μg/ml for brain) and Western blotting using anti–prion protein mAb BAR224 (Cayman Chemical) conjugated to HRP. Blots were developed using chemiluminescent substrates H_2O_2 and luminol for 5 min at room temperature and visualized using a GE digital imager and ImageQuant software. Tissues negative for PrP^{Sc} on Western blots were subjected to serial protein misfolding cyclic amplification (sPMCA) (21). Briefly, protein misfolding cyclic amplification (PMCA) uses 10% NBH in PMCA buffer (1× PBS, 1% Triton X-100, 4 mM EDTA, and 150 mM NaCl) from PrP^{C}-overexpressing transgenic mice, strain TgA20, as substrate for amplification of previously undetectable prions. We mixed 25 μl of NBH with 25 μl of 10% sample homogenate and sonicated samples for 40 s at ~150 W, followed by a 30-min incubation; we repeated this cycle for 24 h, which constituted one round of PMCA. Serial rounds were set up similarly, transferring 25 μl of the previous round's sample to 25 μl of fresh NBH. Each biological sample was run in at least technical duplicates, and round-to-positivity was determined by PK digestion and Western blotting. Relative PMCA units (rpu) were assigned as previously described (22). Nonamplified samples containing detectable PrP^{Sc} via Western blot were assigned a conservative amplification factor of 10 (equating to 1000 rpu) because we estimate that one round of PMCA amplifies PrP^{Sc} ≥10-fold (23).

Histology

Paraffin-embedded 5-μm sagittal brain sections were incubated in 53°C for 30 min prior to immersion in xylene for 10 min and repeated once. Sections were then rehydrated through an ethanol gradient consisting of 100, 95, and 70% concentrations for 5 min each and immersed in 88% formic acid for 10 min. Slides were rinsed in running water for 10 min and autoclaved at 121°C for 2 h in citrate buffer (pH 7.4). Cooled slides were rinsed twice in PBS containing 0.1% Triton X for 5 min on a rocker. To extinguish exogenous peroxidase activity of the tissues, sections were immersed in a 3% H_2O_2 in methanol for 30 min before undergoing another rinse cycle. Tissues were encircled with a DAP pen and incubated with Superblock (Thermo Fisher Scientific) for 30 min. Excess Superblock was removed, and slides were incubated overnight at 4°C with 1:1000 D18 monoclonal Ab recognizing PrP. Slides were rinsed in PBS and incubated with a biotinylated anti-human Ig (1:1000) for 1 h at room temperature. They were then rinsed and incubated with an avidin-biotin complex for 30 min at room temperature. After three rinse cycles, slides were incubated with diaminobenzidine reagent for 2 min, rinsed twice for 2 min with PBS, counterstained with hematoxylin for 5 min, and immersed in water for 10 min. Glial fibrillary acidic protein (GFAP) was detected using rabbit polyclonal antisera against GFAP (diluted 1:8) for 10 min at 37°C followed by biotinylated goat anti-rabbit Ig (mouse/rat adsorbed) for 8 min, and then it was counterstained with hematoxylin for 4 min. Slides were dehydrated through the ethanol gradient and xylene before being mounted with a coverslip. Sections were visualized and digitally photographed using an Olympus BX60 microscope equipped with 10× and 40× objectives and a cool charge-coupled diode camera.

Prion rod preparation and SPR

Prion rods were enriched from infected brain, as previously described (24–27). Briefly, brains from hamsters (5) infected with HY- or DY-transmissible spongiform encephalopathies were homogenized in 1× PBS to 10% (w/v) concentration. Sucrose (1.2 M) was added to 10 ml of clarified tissue to a final concentration of 165.5 mM, and samples were ultracentrifuged (100,000 × *g*) for 1 h at 4°C. Pellets were resuspended to a final protein concentration of 5.0 mg/ml in 1× TBS containing 2.0% Triton X and incubated on ice for 30 min. Samples were subjected to another round of ultracentrifugation for 20 min at 0°C and washed twice with 1× TBS containing 2.0% Triton X and twice with 1× TBS. The

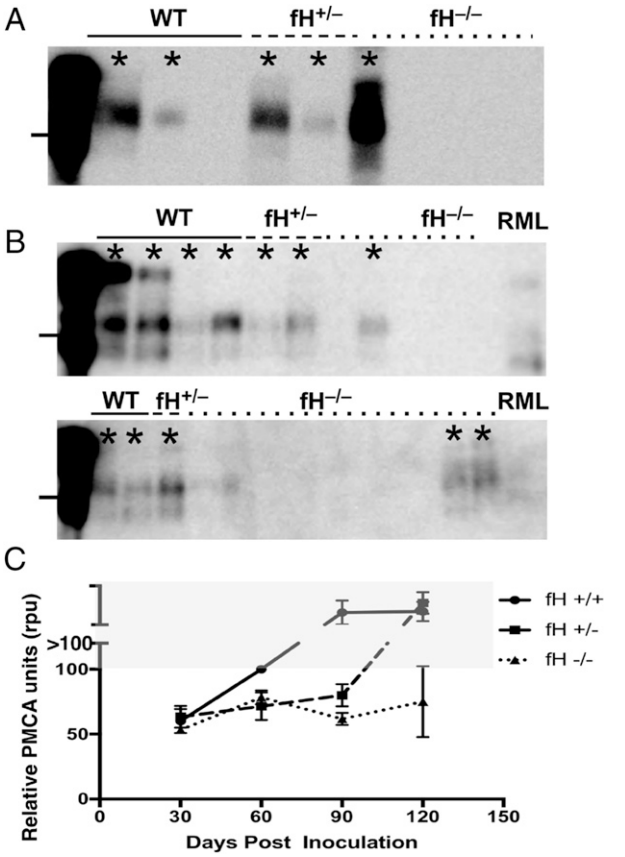

FIGURE 1. fH promotes early prion propagation in spleen at early time points. (**A**) Mice ($n \geq 6$ mice per genotype of both sexes) were sacrificed at 30, 60, 90, and 120 dpi, and their spleens (10% w/v homogenates) were treated with PK (10 μg/ml). Lines to the left of each blot mark 25 kDa m. w. RML-infected animals negative for PrP^{Sc} after straight Western blotting (A) were subjected to serial rounds of PMCA (**B** and **C**). Asterisks indicate samples scored as positive for PrP^{Sc}. Each biological replicate was run in technical duplicates, and each lane represents one mouse. (B) Western blot analysis of PMCA material shows a higher proportion of RML-infected wild-type (WT) mice (solid line) positive by round one of PMCA (upper blot), whereas most knockout mice (lower blot, dotted line) required two or more rounds of PMCA to visualize PrP^{Sc}. RML (far right) represents 0.05% RML5 amplified prions and serves as a positive control for each PMCA round. ANOVA analysis revealed no significant differences at 30 dpi, but significant differences were noted between the genotypes at 60, 90, and 120 dpi ($p = 0.0236$, 0.0021, and 0.0032, respectively). Samples in the first lane of each blot were not digested by PK. (C) Numbers > 100 rpu (gray area of the graph) represent scores from samples detected without amplification and, therefore, fall outside the dynamic range of PMCA.

pellets were then resuspended in 1× PBS containing 1% sarkosyl and protease inhibitor mixture (Roche). Vortexed samples were incubated on a heated shaker at 37˚C for 2 h at 800 rpm. Samples were then gently overlaid on a 0.32 M sucrose in PMCA buffer (PMCA buffer without Triton-X 100) cushion and ultracentrifuged for 1 h at 4˚C, and supernatants were removed. Pellets were resuspended in 2.3 M NaCl, 5% sarkosyl in 1× PBS, centrifuged at 13,000 × *g*, washed three times in 50 mM Tris 150 mM NaCl, and stored dry or suspended in PBS at −80˚C. The presence of PK-resistant prion rods was confirmed by Western blot.

Highly enriched prion rods were coupled to CM-5 sensor chips outside of the instrument after generating the reference flow cells within the instrument by activating with 0.2 M 1-ethyl-3-(3-dimethylaminopropyl) carbodiimide hydrochloride and 0.05 M *N*-hydroxysuccinimide and deactivating with 1 M ethanolamine three to five times. The chip was then removed from the instrument, and the gold chip was disassembled from the cassette. The entire surface was activated with 100 μl of 0.2 M 1-ethyl-3-(3-dimethylaminopropyl) carbodiimide hydrochloride and 0.05 M *N*-hydroxysuccinimide for 12 min. A pellet of rods was resuspended in 100 μl of 10 mM sodium acetate (pH 5.5), sonicated at 37˚C for 40 s, and incubated on the gold chip at room temperature for 1 h. The chip was then briefly rinsed with 1× PBS, and the remaining active groups were deactivated with ethanolamine for 7 min. Prior to use in interaction analyses, four startup cycles of 50 mM sodium hydroxide served to remove any nonspecifically bound prion rods from the surface. Purified C3 and fH were buffer exchanged into 1× running buffer (50 mM Tris base, 150 mM NaCl [pH 7.42]), and protein concentration was determined by protein A280. fH (5, 10, 100, 100, 500, 1000, and 2000 nM) and C3 (5 μM) were passed over HY- or DY-coated CM5 Series S sensor chips for 180 s at 30 μl/min, followed by a 360-s dissociation phase. Affinity analyses were performed using Biacore T200 evaluation software. Baseline = 0 relative response units. Binding levels with mAb BAR224 (200 nM; Cayman Chemical) confirmed that equal amounts of prion amyloid were coated onto each chip.

All SPR experiments involved rPrP or prion rods enriched from infected brain as the ligand coated to a CM5 Series S sensor chip and commercially available fH (CompTech) as the analyte. fH was buffer exchanged in Amicon filter devices into 1× Running Buffer (50 mM Tris HCl, 150 mM NaCl [pH 7.42]). The rPrP-coated chip was kindly provided by Dr. H.-E. Kang of the Telling laboratory.

Statistical analyses

All statistical analyses were performed using GraphPad Prism software. One- or two- way ANOVA was run to compare genotype, sex, or the interaction between these two variables. The p values <0.05 were considered significantly different. In the terminal disease study, we observed one male outlier and subsequently removed this data point. All graphs represent mean ± SEM.

Results

fH promotes early splenic prion propagation

To assess the role of fH in early scrapie trafficking and lymphoid propagation, we inoculated littermates of various *Cfh* genotypes

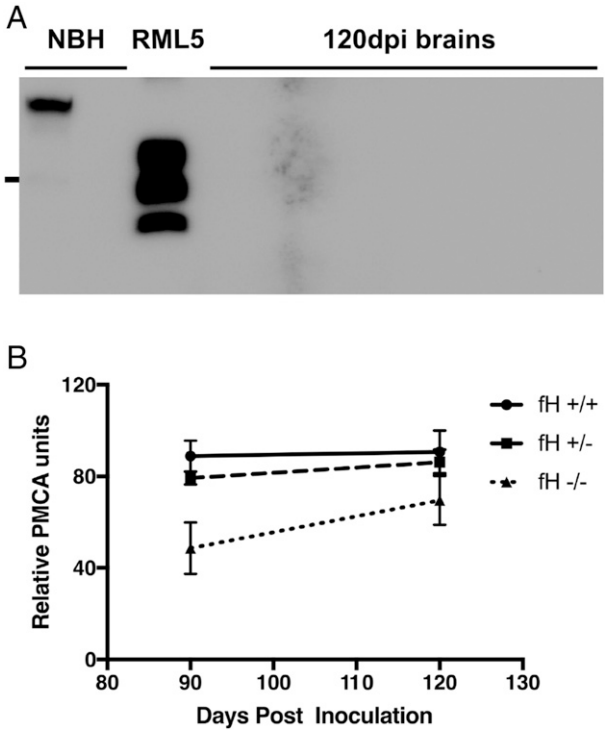

FIGURE 2. fH promotes early prion propagation in brain at early time points. (**A**) Mice ($n \geq 6$ mice per genotype of both sexes) were sacrificed at 60, 90, and 120 dpi, and 10% (w/v) homogenates of their brains were probed for PrP^{Sc}. We detected no PrP^{Sc} by direct Western blotting and, thus, performed sPMCA on all samples. The blot shows representative samples from mice sacrificed at 120 dpi. All samples were digested with PK, with the exception of lane 1. (**B**) Each biological replicate was run in technical duplicates. ANOVA analysis revealed a significant difference at 90 dpi ($p = 0.0024$). Although ANOVA analysis revealed no significant difference at 120 dpi, the unpaired t test revealed significant differences ($p = 0.0269$) between wild-type and knockout PMCA scores.

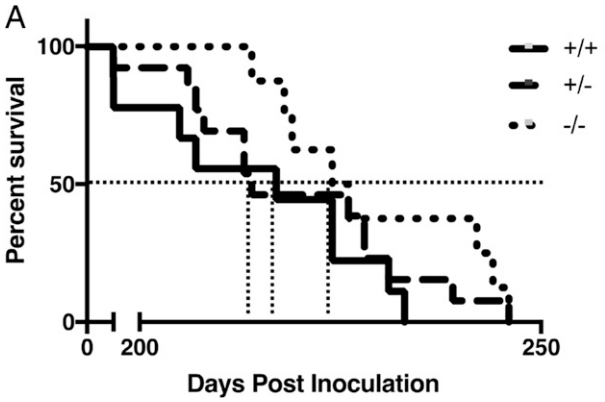

B

Genotype	Sex	Attack Rate	Mean DPI ± sd
fH +/+	M	5/5	222 ± 14
	F	5/5	207 ± 7
fH +/-	M	9/9	222 ± 16
	F	4/4	215 ± 8
fH -/-	M	4/4	238 ± 13
	F	4/4	221 ± 6

FIGURE 3. fH deficiency delays terminal prion disease. Mice of blinded *Cfh* genotype received a single i.p. dose of RML5 scrapie prions and were euthanized at the onset of terminal disease, after which genotype and prion disease were confirmed. Statistical analysis (Mantel-Cox) accounting for sex and genotype revealed a significant difference between survival curves (**A**) ($p = 0.0018$) and mean dpi to terminal disease (**B**) for $fH^{-/-}$ and $fH^{-/+}$ mice of individual ($p = 0.002$) and combined ($p = 0.047$) sexes.

i.p. with 10^6 LD_{50} units of RML5 and assessed prion loads in spleens via PMCA. rpus were assigned as previously described (22). Samples are assigned rpu scores based on the first positive indication of PMCA by detection of amplified prions by Western blot. Samples requiring fewer PMCA rounds to reach the detection threshold receive higher rpu scores. We found that increased splenic loads corresponded with increased *Cfh* gene dosage after 30 d postinfection (dpi) (Fig. 1). Wild-type fH-sufficient mice contained increasing splenic prion loads over time until reaching a plateau load by 90 dpi. Hemizygous mice displayed a lag phase, containing significantly fewer splenic prions than wild-type mice at 60 and 90 dpi and then harboring prion loads similar to wild-type mice by 120 dpi. Completely fH-deficient mice exhibited significantly more protracted prion accumulation at these time points. We detected similar prion loads in mice of all genotypes by 150 dpi (data not shown).

fH promotes prion neuroinvasion

To determine the effects of fH on neuroinvasion, we assessed prion loads in brain at 90 and 120 dpi using sPMCA. Similar to the trend observed in spleen after i.p. challenge, prion loads in the brain positively correlated with *Cfh* expression. fH-deficient mice contained significantly lower prion loads in brain at 90 and 120 dpi (Fig. 2). Interestingly, however, knockout mice reached hemizygous and wild-type brain prion levels by 150 dpi as well.

Absence of fH delays clinical manifestations of terminal prion disease and affects prion-deposition patterns

In a blind-to-genotype study, we challenged littermates with a single peritoneal dose of RML5 and monitored them daily for onset of clinical disease (Fig. 3). Aligning with early accumulation studies, $fH^{-/-}$ mice resisted the onset of terminal prion disease significantly longer than did $fH^{-/+}$ and wild-type mice. We also noted a significant sex difference among the different genotypes, with male mice resisting terminal prion disease longer than females.

Histological examination of brains from these mice confirmed neuropathology consistent with terminal prion disease, including astrogliosis, vacuolation, and PrP^{Sc} deposition (Fig. 4). In mice expressing fH, we consistently observed typical diffuse PrP^{Sc} staining indicative of the RML5 mouse–adapted prion strain. However, in a subset of fH-deficient mice we observed striking differences in PrP^{Sc} deposition patterns that included florid plaques, numerous puncta, and even PrP^{Sc} contained in intracellular structures reminiscent of inclusion bodies.

fH directly binds PrP^C and prion amyloid

Previous reports indicate a molecular interaction between various conformations of rPrP and fH, but whether fH bound in vivo–derived prion amyloid remained unknown. Therefore, we used SPR to test the interaction of fH with highly enriched prion rods isolated from hamsters infected with two distinct strains of TME prions; the HY strain is lymphotropic, whereas the DY strain is not. fH bound the lymphotropic HY strain with slightly higher affinity (310 nM) than the DY TME strain (343 nM) (Fig. 5).

Discussion

We investigated the influence of complement regulatory protein fH in establishing prion infection after peripheral insult. Our data show that fH directly binds prions and promotes splenic propagation, neuroinvasion, and terminal disease onset. Although $fH^{-/-}$ mice eventually succumbed to prion disease, lymphotropism and sub-

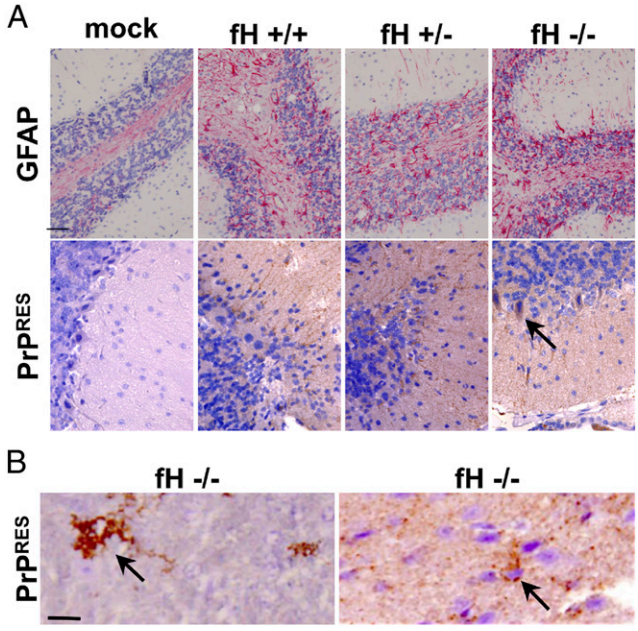

FIGURE 4. fH-knockout mice contain unique PrP^{Sc}-deposition profiles. Spleen sections were stained with Abs recognizing GFAP and PrP^{Sc}, then counterstained with hematoxylin. (**A**) Infected mice of all genotypes displayed prion neuropathology, including astrogliosis and PrP^{Sc} deposition. No prion deposition was observed in mock-infected mice. All infected fH wild-type and hemizygous mice contained typical diffuse RML5 deposition, whereas fH-deficient mice contained cerebellar prion deposition suggestive of inclusion bodies at terminal disease (lower panels). (**B**) We observed florid plaques (left panel) and puncta (right panel) in a subset of fH-knockout mice. Arrows point to prion deposition unique to fH-knockout mice. Scale bars, 100 μm.

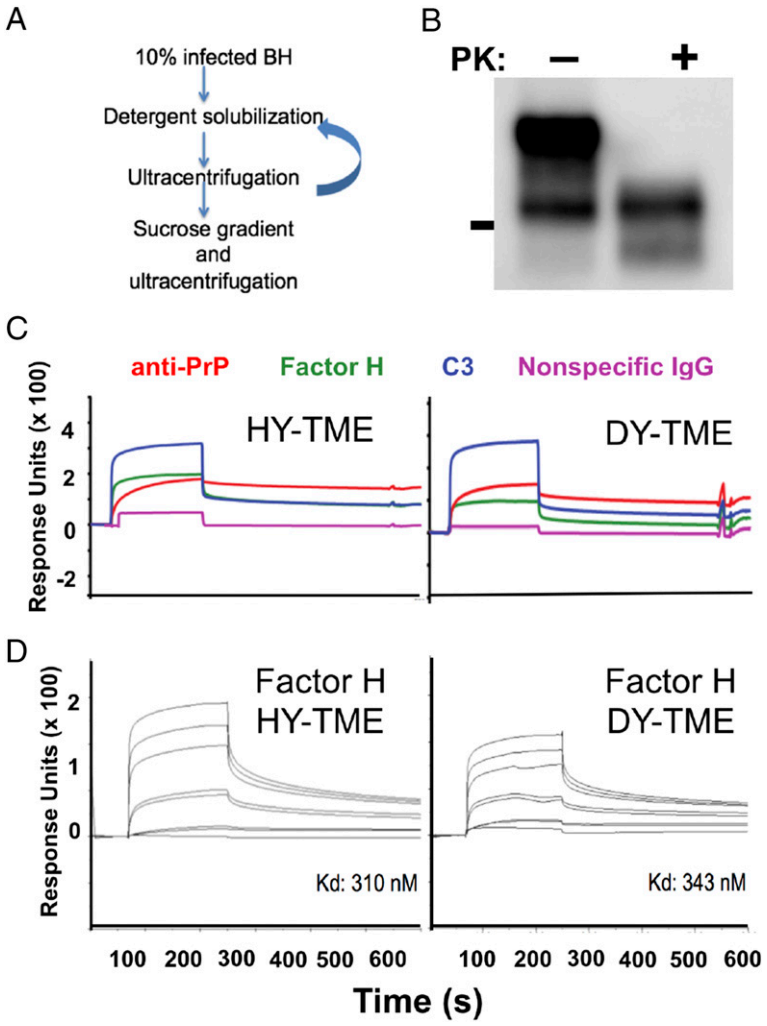

FIGURE 5. fH interacts directly with prion amyloid enriched from infected brain. Prion rods were enriched from infected brains as previously described (**A**) and are PK resistant (**B**). The line to the left of the blot marks 25 kDa m.w. (**C**) fH interacts biochemically with prion rods of HY and DY strains manually coupled to an SPR sensor chip. (**D**) Affinity analyses show that fH bound HY prions with slightly higher affinity than DY prions. Traces from the bottom to the top of the sensorgrams show binding of 0, 5, 10, 100, 100, 500, 1000, and 2000 nM fH analytes to prions coated on the chip.

sequent neuroinvasion were impaired. Interestingly, splenic prion burdens did not differ between genotypes at 30 dpi. These data reveal no differences in initial trafficking of inocula to spleens, but impaired prion replication during the nonclinical phase of disease, suggesting that fH may stabilize prions or promote propagation once captured in the lymphoreticular system. We previously showed that prions could traffic to lymphoid tissues cell autonomously (26), independent of an intact complement system. Perhaps soluble fH acts as a transport chaperone for such autonomous prions. Assessing the effects of pretreating prion inocula with fH on early cell-mediated and cell-autonomous prion trafficking, as well as degradation, could help to test this hypothesis. We observed no differences in splenic prion accumulation or neuroinvasion by 150 dpi.

We can envision several roles for fH in directly promoting prion disease. As discussed above, fH could act as a soluble prion receptor and cell autonomously shuttle prions to extraneural sites of prion replication. Alternatively, or even additionally, fH bound to PrP^C-expressing cells could capture prions, bringing them to the vicinity of PrP^C molecules, which then misfold and join the growing prion aggregate. Furthermore, fH may preferentially bind prions adopting distinct conformations or possessing certain post-translational modifications, thereby selecting for certain strains to replicate in the lymphoreticular system.

Previous studies using mouse models of scrapie (9, 13) and chronic wasting disease (12) reveal that mice genetically or pharmacologically deficient in C3 accumulate fewer prions and resist terminal disease longer than their C3-sufficient controls. Prion opsonization likely promotes local degradation of prions by macrophages, as well as trafficking to and subsequent propagation in lymphoid tissues, hallmark areas of early prion replication. fH deficiency results in increased C3 convertase formation and causes unregulated cleavage of C3 and downstream depletion of serum C3 (15). However, Klein et al. (9) reported no difference in progression to terminal prion disease in C3-deficient and wild-type mice upon a high-dose challenge. In this article, we report a significantly delayed onset of terminal prion disease upon high-dose challenge in mice lacking fH and, therefore, C3, compared with wild-type mice. Thus, fH deficiency likely plays a more substantial role in prolonging prion disease than simply eliminating C3.

Complement control proteins contain highly homologous series of 60–70 aa termed short consensus repeats (SCRs). SCRs recognize certain C3/C4 cleavage products, and each complement control protein elicits distinct downstream functions. For example, complement receptor 2 (CR2 or CD21) recognizes opsonized pathogens via its SCRs and reduces the threshold of B cell activation, whereas fH recognizes sialylated host products via its SCRs to prevent autoimmunity. Essentially, these proteins stimulate opposing effects using highly homologous SCRs. Domain-mapping studies in our laboratory reveal CD21 containing the first two SCRs is sufficient to recognize prion amyloid (S.J. Kane and M.D. Zabel, manuscript in preparation). Therefore, we conclude that CD21 is a cell surface prion receptor that facilitates

prion propagation in lymphoid tissues prior to neuroinvasion. We propose that fH is both a soluble and cell-associated prion receptor and assists in prion disease, similarly to CD21. Therefore, we conclude that SCRs on complement control proteins, such as CD21 and fH, bind prions either cell mediated or cell autonomously and promote lymphotropism and subsequent neuroinvasion.

Sjöberg et al. (19) reported that fH biochemically interacts with various conformers of prion protein but preferentially bound oligomeric species. Amyloid plaques, in Alzheimer's disease and prion diseases, appear to be relatively innocuous forms of the misfolded protein, whereas oligomeric species cause the cytotoxic features (27). It is possible that oligomeric species, as a result of their smaller size and less amyloidogenic status, are more sensitive to protease or cell-mediated degradation. fH may bind, thereby protect, and shuttle protease-sensitive oligomers to extraneural sites where oligomers could propagate into, and perhaps even seed, amyloid production. We show that fH binds the lymphotropic HY strain with slightly higher affinity than the nonlymphotropic DY prion strain. However, this slight affinity difference likely does not fully explain lymphotropic differences for these strains. Furthermore, these studies only test interactions with prion amyloid derived from hamster brain. Whether fH differentially binds HY TME or DY TME oligomeric species remains undetermined, as does whether fH differentially binds RML5 mouse prions, primarily as a result of the difficulty in isolating sufficient RML5 prion rods from mouse brains to perform those analyses. HY and DY hamster prions likely form conformations distinct from RML5 mouse prions, another lymphotropic strain used in these infection studies. We predict, based on the in vivo infection studies reported in this article, that fH binds RML5 prions as well. We are currently investigating the role of fH in prion strain selection, stabilization, and trafficking in vivo.

Baskakov and colleagues (28, 29) convincingly demonstrated that sialylation status differs among prion strains, which could dictate fH binding. Katorcha et al. (30) reported that PrP^{Sc} sialylation increased prion infectivity. PMCA-generated material derived from desialylated substrate did not infect wild-type mice, whereas PMCA-generated material from fully sialylated substrate resulted in a 100% infection rate. fH may bind sialylated PrP^{Sc} and facilitate disease via the shuttling mechanism described above. Hepatocarcinoma cells use sialic acids to selectively adhere to secondary lymphoid organs (reviewed in Ref. 29). Perhaps fH aids sialylated prions in infecting lymphoid organs via a similar mechanism. Accordingly, desialylated PMCA material was undetectable in spleen or brain after serial rounds of PMCA, which is indicative of degradation or urinary or fecal secretion. Perhaps fH could explain both observations by binding sialic acid on cancerous cells and prions, resulting in evasion of cellular destruction and granting entry to lymphoid tissues.

fH could also be involved in selecting different prion strains to be propagated in lymphoid organs by preferentially binding sialylated prions. Although we show in this article that fH binds lymphotropic and nonlymphotropic strains, their sialylation status is unknown. fH has also been shown to bind rPrP free of posttranslational modifications (19, 20) and, therefore, may dictate prion strain selection and disease outcomes independent of, or in addition to, sialylation status. Qualitative histological examination revealed that a higher proportion of $fH^{-/-}$ mice contained florid or intracellular prion deposition/accumulation versus the typical and extremely consistent diffuse RML5 deposition in wild-type mice (Fig. 4), supporting the hypothesis that fH is a key host factor in prion strain selection. Additionally, soluble fH may prevent certain prion strains, like RML5, from aggregating into puncta, causing diffuse prion deposition.

Altogether, these data support a role for fH in peripheral prion disease pathogenesis by directly interacting with infectious prions and promoting lymphotropism and subsequent neuroinvasion. We propose that fH selects for certain prion strains. Whether this prion selection occurs at the level of prion conformation, sialylation status, degradation evasion, or a combination of these processes remains to be determined.

Acknowledgments

We thank Dr. Hae-Eun Kang for aid and consultation in the SPR experiments, Joshua Thurman for breeding pairs of fH-deficient mice, and Jason Bartz for hamster brains.

Disclosures

The authors have no financial conflicts of interest.

References

1. Somerville, R. A., C. R. Birkett, C. F. Farquhar, N. Hunter, W. Goldmann, J. Dornan, D. Grover, R. M. Hennion, C. Percy, J. Foster, and M. Jeffrey. 1997. Immunodetection of PrPSc in spleens of some scrapie-infected sheep but not BSE-infected cows. *J. Gen. Virol.* 78: 2389–2396.
2. Bartz, J. C., C. Dejoia, T. Tucker, A. E. Kincaid, and R. A. Bessen. 2005. Extraneural prion neuroinvasion without lymphoreticular system infection. *J. Virol.* 79: 11858–11863.
3. Bessen, R. A., and R. F. Marsh. 1992. Biochemical and physical properties of the prion protein from two strains of the transmissible mink encephalopathy agent. *J. Virol.* 66: 2096–2101
4. Béringue, V., L. Herzog, E. Jaumain, F. Reine, P. Sibille, A. Le Dur, J. L. Vilotte, and H. Laude. 2012. Facilitated cross-species transmission of prions in extraneural tissue. *Science* 335: 472–475.
5. Montrasio, F., R. Frigg, M. Glatzel, M. A. Klein, F. Mackay, A. Aguzzi, and C. Weissmann. 2000. Impaired prion replication in spleens of mice lacking functional follicular dendritic cells. *Science* 288: 1257–1259.
6. Brown, K. L., K. Stewart, D. L. Ritchie, N. A. Mabbott, A. Williams, H. Fraser, W. I. Morrison, and M. E. Bruce. 1999. Scrapie replication in lymphoid tissues depends on prion protein-expressing follicular dendritic cells. *Nat. Med.* 5: 1308–1312.
7. Zabel, M. D., M. Heikenwalder, M. Prinz, I. Arrighi, P. Schwarz, J. Kranich, A. von Teichman, K. M. Haas, N. Zeller, T. F. Tedder, et al. 2007. Stromal complement receptor CD21/35 facilitates lymphoid prion colonization and pathogenesis. *J. Immunol.* 179: 6144–6152.
8. McCulloch, L., K. L. Brown, B. M. Bradford, J. Hopkins, M. Bailey, K. Rajewsky, J. C. Manson, and N. A. Mabbott. 2011. Follicular dendritic cell-specific prion protein (PrP) expression alone is sufficient to sustain prion infection in the spleen. *PLoS Pathog.* 7: e1002402.
9. Klein, M. A., P. S. Kaeser, P. Schwarz, H. Weyd, I. Xenarios, R. M. Zinkernagel, M. C. Carroll, J. S. Verbeek, M. Botto, M. J. Walport, et al. 2001. Complement facilitates early prion pathogenesis. *Nat. Med.* 7: 488–492.
10. Klein, M. A., R. Frigg, A. J. Raeber, E. Flechsig, I. Hegyi, R. M. Zinkernagel, C. Weissmann, and A. Aguzzi. 1998. PrP expression in B lymphocytes is not required for prion neuroinvasion. *Nat. Med.* 4: 1429–1433
11. Michel, B., A. Ferguson, T. Johnson, H. Bender, C. Meyerett-Reid, B. Pulford, A. von Teichman, D. Seelig, J. H. Weis, G. C. Telling, et al. 2012. Genetic depletion of complement receptors CD21/35 prevents terminal prion disease in a mouse model of chronic wasting disease. *J. Immunol.* 189: 4520–4527.
12. Michel, B., A. Ferguson, T. Johnson, H. Bender, C. Meyerett-Reid, A. C. Wyckoff, B. Pulford, G. C. Telling, and M. D. Zabel. 2013. Complement protein C3 exacerbates prion disease in a mouse model of chronic wasting disease. *Int. Immunol.* 25: 697–702.
13. Mabbott, N. A., M. E. Bruce, M. Botto, M. J. Walport, and M. B. Pepys. 2001. Temporary depletion of complement component C3 or genetic deficiency of C1q significantly delays onset of scrapie. *Nat. Med.* 7: 485–487.
14. Carroll, M. V., and R. B. Sim. 2011. Complement in health and disease. *Adv. Drug Deliv. Rev.* 63: 965–975.
15. Pickering, M. C., H. T. Cook, J. Warren, A. E. Bygrave, J. Moss, M. J. Walport, and M. Botto. 2002. Uncontrolled C3 activation causes membranoproliferative glomerulonephritis in mice deficient in complement factor H. *Nat. Genet.* 31: 424–428
16. Zipfel, P. F., M. Edey, S. Heinen, M. Józsi, H. Richter, J. Misselwitz, B. Hoppe, D. Routledge, L. Strain, A. E. Hughes, et al. 2007. Deletion of complement factor H-related genes CFHR1 and CFHR3 is associated with atypical hemolytic uremic syndrome. *PLoS Genet.* 3: e41.
17. Hageman, G. S., D. H. Anderson, L. V. Johnson, L. S. Hancox, A. J. Taiber, L. I. Hardisty, J. L. Hageman, H. A. Stockman, J. D. Borchardt, K. M. Gehrs, et al. 2005. A common haplotype in the complement regulatory gene factor H (HF1/CFH) predisposes individuals to age-related macular degeneration. *Proc. Natl. Acad. Sci. USA* 102: 7227–7232.
18. Srivastava, S., N. Makarava, E. Katorcha, R. Savtchenko, R. Brossmer, and I. V. Baskakov. 2015. Post-conversion sialylation of prions in lymphoid tissues. *Proc. Natl. Acad. Sci. USA* 112: E6654–E6662.

19. Sjöberg, A. P., S. Nyström, P. Hammarström, and A. M. Blom. 2008. Native, amyloid fibrils and beta-oligomers of the C-terminal domain of human prion protein display differential activation of complement and bind C1q, factor H and C4b-binding protein directly. *Mol. Immunol.* 45: 3213–3221.
20. Mitchell, D. A., L. Kirby, S. M. Paulin, C. L. Villiers, and R. B. Sim. 2007. Prion protein activates and fixes complement directly via the classical pathway: implications for the mechanism of scrapie agent propagation in lymphoid tissue. *Mol. Immunol.* 44: 2997–3004.
21. Saborio, G. P., B. Permanne, and C. Soto. 2001. Sensitive detection of pathological prion protein by cyclic amplification of protein misfolding. *Nature* 411: 810–813.
22. Pulford, B., T. R. Spraker, A. C. Wyckoff, C. Meyerett, H. Bender, A. Ferguson, B. Wyatt, K. Lockwood, J. Powers, G. C. Telling, et al. 2012. Detection of PrPCWD in feces from naturally exposed Rocky Mountain elk (*Cervus elaphus nelsoni*) using protein misfolding cyclic amplification. *J. Wildl. Dis.* 48: 425–434.
23. Meyerett, C., B. Michel, B. Pulford, T. R. Spraker, T. A. Nichols, T. Johnson, T. Kurt, E. A. Hoover, G. C. Telling, and M. D. Zabel. 2008. In vitro strain adaptation of CWD prions by serial protein misfolding cyclic amplification. *Virology* 382: 267–276.
24. Safar, J., W. Wang, M. P. Padgett, M. Ceroni, P. Piccardo, D. Zopf, D. C. Gajdusek, and C. J. Gibbs, Jr. 1990. Molecular mass, biochemical composition, and physicochemical behavior of the infectious form of the scrapie precursor protein monomer. *Proc. Natl. Acad. Sci. USA* 87: 6373–6377.
25. Johnson, T. E., B. A. Michel, C. Meyerett, A. Duffy, A. Avery, S. Dow, and M. D. Zabel. 2010. Monitoring immune cells trafficking fluorescent prion rods hours after intraperitoneal infection. *J. Vis. Exp.* (45): 2349.
26. Michel, B., C. Meyerett-Reid, T. Johnson, A. Ferguson, C. Wyckoff, B. Pulford, H. Bender, A. Avery, G. Telling, S. Dow, and M. D. Zabel. 2012. Incunabular immunological events in prion trafficking. *Sci. Rep.* 2: 440.
27. Silveira, J. R., G. J. Raymond, A. G. Hughson, R. E. Race, V. L. Sim, S. F. Hayes, and B. Caughey. 2005. The most infectious prion protein particles. *Nature* 437: 257–261.
28. Katorcha, E., N. Makarava, R. Savtchenko, and I. V. Baskakov. 2015. Sialylation of the prion protein glycans controls prion replication rate and glycoform ratio. *Sci. Rep.* 5: 16912.
29. Baskakov, I. V., and E. Katorcha. 2016. Multifaceted role of sialylation in prion diseases. *Front. Neurosci.* 10: 358.
30. Katorcha, E., N. Makarava, R. Savtchenko, A. D'Azzo, and I. V. Baskakov. 2014. Sialylation of prion protein controls the rate of prion amplification, the cross-species barrier, the ratio of PrPSc glycoform and prion infectivity. *PLoS Pathog.* 10: e1004366.